

A WAVELET BASED FLIGHT DATA PREPROCESSING METHOD FOR FLIGHT CHARACTERISTICS ESTIMATION AND FAULT DETECTION

Masaru Naruoka*

***Japan Aerospace Exploration Agency**

Keywords: *Flight analyses, Multiresolution Analysis, Flight characteristics estimation, Fault detection*

Abstract

This paper proposes a new flight data preprocessing method, which add time series data to flight phase indexes. In addition, the method outputs values representing correlation strength among different types of data. The generated information will greatly supports flight characteristics estimation and fault detection, whose performance quite depend on the quality of their input flight data. The effectiveness of the proposed method is demonstrated with these two applications by using the real flight data obtained with fixed-wing aircraft.

1 Introduction

Flight data represented by altitude, airspeed and acceleration is generally obtained in the form of time series data. The time series flight data is not suitable to be analyzed directly, because the data is too enormous to find appropriate parts required by an application. Even if people try to select the appropriate parts manually, it takes much time, and there seems to be error for the selection. Furthermore, existing automatic methods represented by pattern recognition have capability to extract the parts, however, they must prepare specific template experienced in past flights. Therefore, a new preprocessing method to help the selection without specific templates is proposed in this study.

The proposed method provides two func-

tions; phase indexer and correlation measure. The phase indexer is to separate flight data into parts automatically in terms of flight phases and stability. The flight phases are represented by ascending, descending, and horizontal flights, while the stability indicates how abrupt changes are measured. In addition to the phase indexer, the proposed method has the correlation measure, which provides a scale to indicate correlations between different kinds of data. For instance, a large scale value is observed for combination of rolling rate and deflection of fixed-wing aircraft aileron when a turning of the aircraft is started.

The proposed method is initially motivated by utilization for flight characteristics estimation. The estimation generally identifies parameters represented by aerodynamic coefficients and stability derivatives for static and dynamic characteristics, respectively. The accuracy of the estimated parameters quite depends on which flight phase data is used and how strong correlation is recorded on the data. In the worst case, a technique that some parameters are intentionally fixed must be introduced to mitigate effect of noise, which results in inappropriate estimation. Thus, the proposed method, which enables us to select the appropriate flight phases and the strongly correlated parts easily, will be effective for the estimation.

Fault detection has also been focused as an application when the proposed method is studied. This is because the fault detection performance depends on the quality of data to be analyzed like

the estimation performance of the flight characteristics. Especially, when priori information that multiple kinds of data are correlated in a normal case has been already experienced, the fault is more easily detectable by monitoring the correlation rather than by monitoring original time series data carefully. This is clearly understood to consider an example situation that changes of control column inputs of fixed-wing aircraft do not invoke assumed pitching. Therefore, the capability to measure the correlation of the proposed method also will be useful for the detection.

Based on the aforementioned background, the two functions are equipped with the proposed method. In the following, the detail of the proposed method is described in Sec. 2. The method is an extended version of the previous study of the author, and is explained step by step. Then, the effectiveness of the proposed method is demonstrated in Sec. 3. The demonstration is performed with real flight data. The specification of the flight data, and the applications to both the estimation of the flight characteristics and the abnormal detection are elaborated. Finally, conclusion remarks are summarized in Sec. 4.

2 Method

This section describes the details of the proposed method. The proposed method is an improved version of the classifying method [1] studied by the author previously. Figure 1 shows the diagram of the proposed method, and also indicates the previous method indicated by the red bordered square in the figure. In accordance with Fig. 1, the proposed method is explained in the followings.

2.1 Previous method

Firstly, the previously studied method, which divides flight data into just two categories; stable and unstable flights, is described. This classification is performed by using values designated as “signal strength” denoted by a symbol y' in the figure. The signal strength indicates how quick and strong changes are occurred in a certain kind of data and during a certain period. Each signal

strength y' corresponding to time series data during a certain period is calculated as

$$y'_i(j) \equiv \frac{\sum_{k=1}^{2^{i-1}+1} a(j-k) - \sum_{k=0}^{2^i-1} a(j+k)}{2^i}, \quad (1)$$

where subscripts i represents length of the period to be focused, j indicates sample index, and a is time series data. When the signal strength difference between long and short periods

$$\Delta y'(i_{\text{long}}, i_{\text{short}}) \equiv y'_{i_{\text{long}}} - y'_{i_{\text{short}}} \quad (2)$$

is included in a predefined threshold, the previous method classifies a corresponding part as stable.

The computation of the signal strength is continuously and effectively performed with a multiresolution analysis (MRA) [2] block followed by signal conditioner as shown in Fig. 1. The MRA block decomposes signal into both time and frequency domain based on Haar wavelet transform techniques [3]. The cascading application of Haar wavelet transform in the MRA block results in the low computational cost.

The signal conditioner amplifies the outputs of the MRA blocks and delays their propagation. The amplifier gain of the conditioner is tuned for each period treated in the MRA block in order to let the conditioner outputs, that is, the signal strength, have a physical meaning. As Eq. (1) shows, the signal strength y' corresponds to difference of averages, in other words, smoothed gradient. This makes determination of the threshold easier, for example, the threshold for altitude is represented as the difference of rate of climb (RoC).

The delay rate of the conditioner is also carefully configured for each period. This results from that the calculation performed in the MRA block for the longer period requires the more samples. Consequently, the delay insertion enables the conditioner outputs to be synchronized. This synchronization feature is suitable for real-time applications.

2.2 Proposed method

The proposed method more actively uses the difference between the long and short period signal

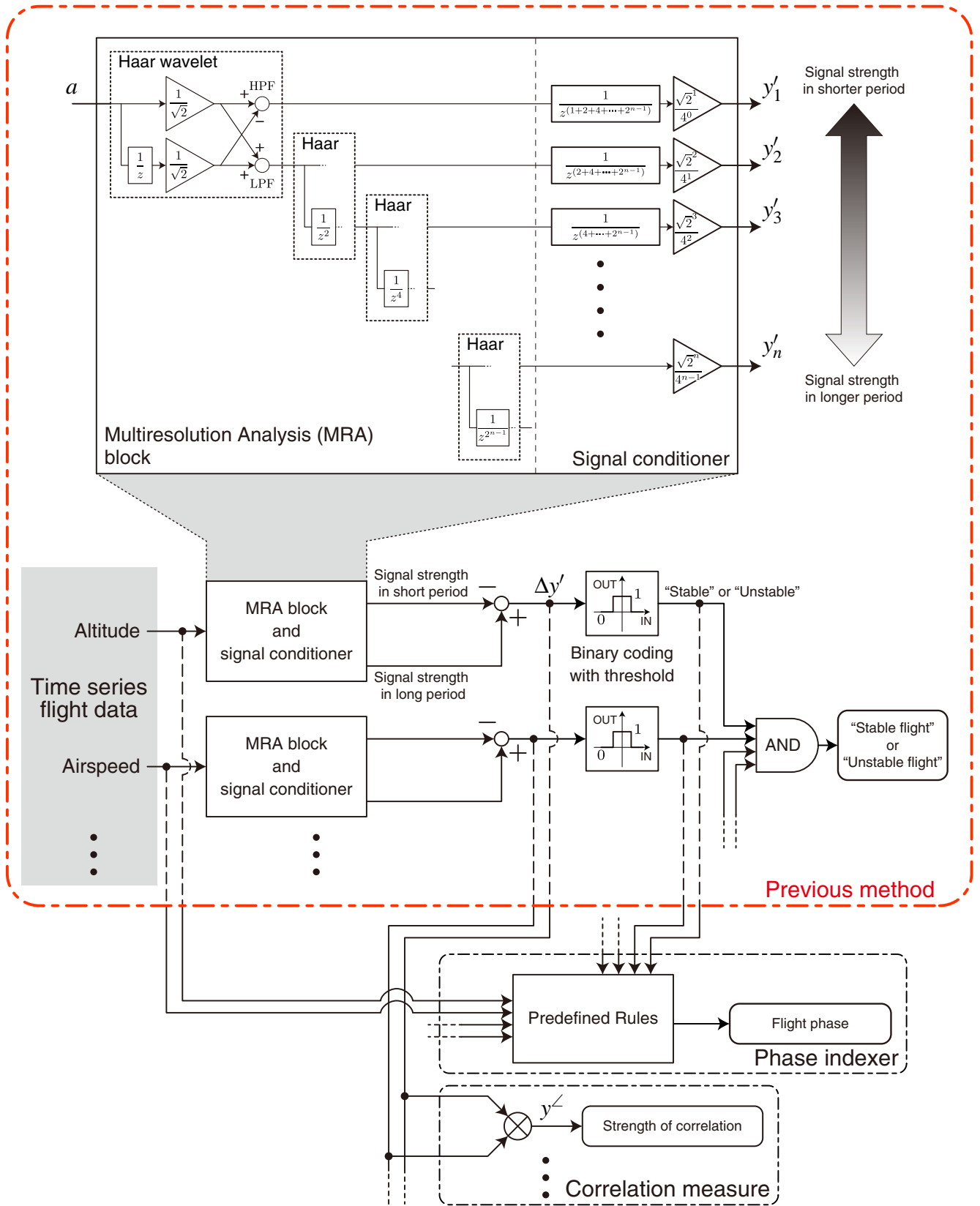


Fig. 1 Processing diagram of the proposed method

strength. The method newly provides two functions; the phase indexer and correlation measure.

The phase indexer enhances the capability of the previous method, which just divide data into the stable and unstable parts. Generally, the stable parts can be easily labeled. For example, ascending, descending, and level phases are easily recognized by monitoring altitude, especially when the altitude change is stable. By using this fact, the phase indexer determines which flight phase current state is belonged to based on predefined rules when changes of corresponding time series data are recognized as sufficiently stable. The predefined rules can be simple, such as, whether the change is increasing or decreasing, because the stability of the changes has been already compensated. Actually, the rules used for applications of the proposed method to fixed-wing aircraft, whose details are described in section 3 are sufficiently simple as Table 1 shows.

The other function, i.e., the correlation measure, is the scale indicating correlation strength between two kinds of time series data. A scale value, which is indicated as a symbol y^{\sphericalangle} in Fig. 1, is calculated by multiplying the signal strength differences as

$$y^{\sphericalangle} \equiv \Delta y'_{\text{item1}} \times \Delta y'_{\text{item2}}. \quad (3)$$

Why this value indicates the correlation strength is clearly understood with a case that when change of two correlated data set is occurred at the same time, both the two signal strength differences take large values, and the corresponding scale value is also large. On the contrary, when two data sets are uncorrelated, even if one of the differences takes a large value, the other is small and the index value will be small.

3 Application demonstrations

The effectiveness of the proposed method is demonstrated with the two applications; flight characteristic estimation and abnormal detection. Firstly, the flight data used for the demonstration is described. Then, primitive results obtained by just applying the proposed method to the flight data are shown, and the fundamental capability

of the proposed method is evaluated. Comprehensive results of the two applications obtained by utilization of the primitive results follow, and the total effectiveness of the method is discussed.

3.1 Flight data and primitive results

The flight data used for the demonstration is collected by research aircraft “Hisho” shown in Fig. 2 owned by Japan Aerospace Exploration Agency (JAXA). This aircraft was originally Cessna 680 Citation Sovereign, which is fixed wing, twin turbojet powered aircraft, and has been modified for various research flight. As one of the modifications, 270 kinds of data are recorded during flight with network-based data acquisition system [4]. The representatives of the data are navigation information such as position, velocity and attitude, air data consisting of air-speed, angle of attack, and pressure altitude, and engine operating status captured with full authority digital engine control (FADEC). Control inputs varying from control stick positions to control surface deflections are also acquired. Aircraft weight and thrust force can be estimated with the directly obtained data represented by fuel flow and fan speed (N1) of FADEC. The sampling frequency of the data varies among the data source, and its maximum reaches 50 Hz for navigation information. In this study, the data to be analyzed by the proposed method is down-sampled to 10 Hz for reduction of computational load.



Fig. 2 Research aircraft “Hisho”

For the demonstration, flights belonging to two categories A and B are selected. Category A flight is a normal flight, in which the aircraft takes off an airport and lands to another airport with ordinary maneuvering. Category B flight is an experimental flight, in which the aircraft is intentionally swayed in order to invoke characteristic motion represented by phugoid and dutchroll.

Table 1 Predefined rules for the phase indexer

Item (Symbol)	Rules
Pressure altitude (h)	<i>if</i> $ \Delta h/\Delta t \leq 100$ fpm <i>then</i> “level flight”, <i>else if</i> $(\Delta h/\Delta t) > 100$ fpm <i>then</i> “ascending”, <i>else</i> “descending”.
True airspeed (V_{TAS})	<i>if</i> $ \Delta V_{TAS}/\Delta t \leq 0.1$ kts <i>then</i> “constant airspeed”, <i>else if</i> $(\Delta V_{TAS}/\Delta t) > 0.1$ kts <i>then</i> “accelerating”, <i>else</i> “decelerating”.
True heading (ψ)	<i>if</i> $ \Delta \psi \leq 1$ deg <i>then</i> “straight flight”, <i>else if</i> $\Delta \psi > 1$ deg <i>then</i> “right turn”, <i>else</i> “left turn”.

[†] Δx shown in the above table represents a difference between initial and last x in a period recognized as stable. t is time, namely, Δt is length of the stable period.

Many coordinated turns are also performed in the category B flights. The numbers of category A and B flights are 4 and 3, and the length are approximately 11 and 13 hours, respectively.

Figures 3 and 4 are data obtained in one of the category A and B flights, respectively. In the figures, the time histories of pressure altitude, true airspeed, true heading and roll angle, which will be analyzed with the proposed method, are depicted. The other category A and B flights, whose data are not displayed due to the paper space limitation, have the same tendency of change as Figs. 3 and 4 show.

The proposed method is applied with the predefined rules for the phase indexer summarized in table 1 to these flight data. In Figs. 3 and 4, the signal strength differences are also indicated. The thresholds for determination of whether flight is stable or unstable are depicted as horizontal dashed lines. The phase indexer results are shown as hatched area in each time histories; colored areas are recognized as stable flights, and each color corresponds to each indexed flight phase. Table 2 summarizes the length of the flight phase labeled by the phase indexer.

According to Figs. 3 and 4, it seems that the phase indexer of the proposed method sufficiently works. Especially, the difference between category A and B flights are highlighted by the method recognizing category A flights are more stable than category B flights. Table 2 also supports this fact quantitatively; the ratio occupied

by the level straight flights with constant airspeed is far higher in category A flights compared to category B Flights, which actually characterizes the both category flights.

Table 2 Length of indexed flight phase

Item	Flight category	
	A	B
(Total)	39867.9	46526.4
Stable	17600.3	6102.4
Level flight ¹	12275.3	4092.0
Ascending ¹	882.9	82.7
Descending ¹	584.3	881.4
Constant airspeed ²	12579.9	4027.5
Accelerating ²	437.6	354.0
Decelerating ²	443.6	674.6
Straight flight ³	17248.7	3441.9
Right turn ³	230.2	1396.3
Left turn ³	121.4	1264.2

[†] Dimensions are in seconds.

¹ Level flight, ascending, and descending are displayed as green, blue and red colored areas in the pressure altitude graphs of Figs. 3-4.

² Constant airspeed, accelerating, and decelerating are displayed as green, red and blue colored areas in the true airspeed graphs of Figs. 3-4.

³ Straight flight, right, and left turns are displayed as green, red and blue colored areas in the heading graphs of Figs. 3-4.

The representative result obtained by the correlation measure is depicted in Fig. 5. The graphs in the figure show a heading change in one of the category A flights, which corresponds to the part

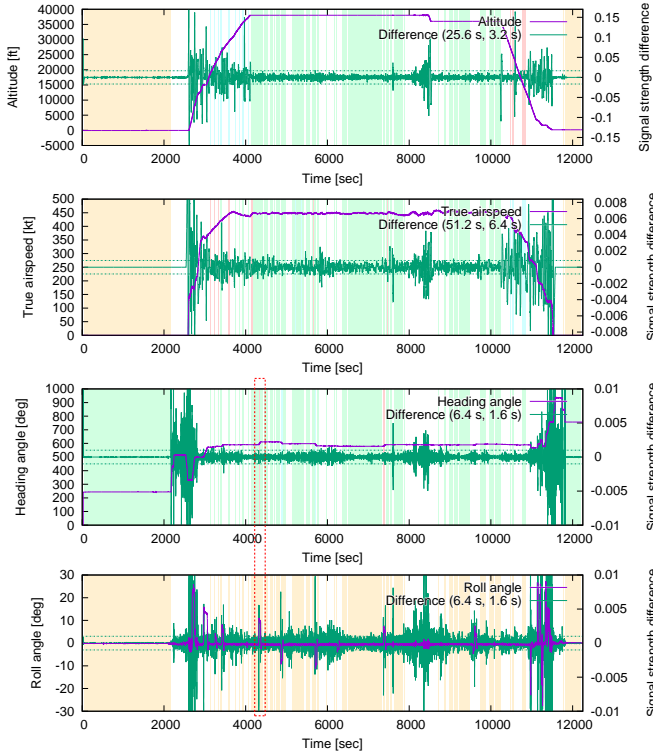


Fig. 3 Category A “normal” flight data (Flight No. A130930)

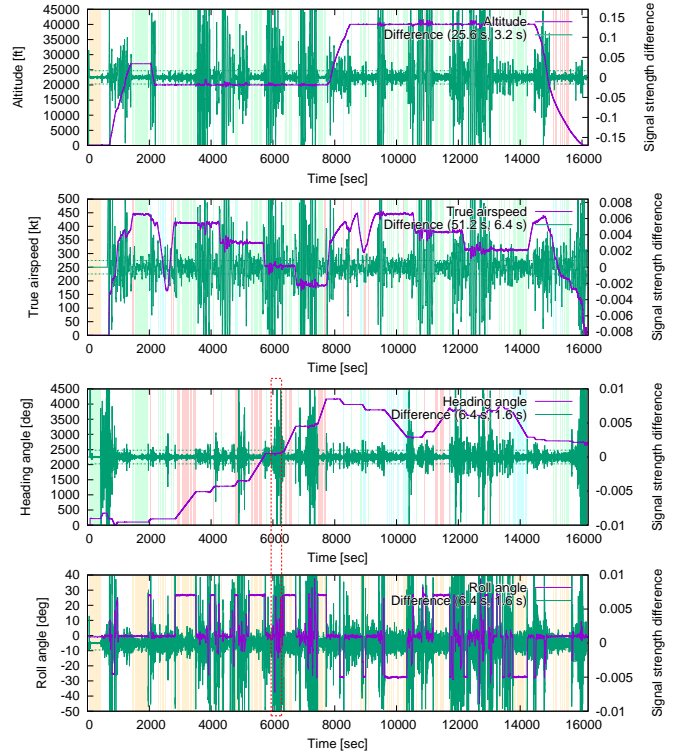


Fig. 4 Category B “experimental” flight data (Flight No. B160617)

surrounded by the red dashed box in Fig. 3. The time history of the correlation strength of heading and aileron position calculated with the correlation measure is displayed in addition to the time histories of heading, roll angle, and aileron position. The time history of rudder position and its correlation strength are also included in the figure. The larger scale values are monitored in the correlation strength between the heading and aileron position compared to that between the heading and rudder position when the heading change is initiated and terminated, which indicates that not the rudder but the aileron is manipulated to change the heading. This is natural maneuvering for the fixed-wing aircraft, and shows the fundamental effectiveness of the correlation measure of the proposed method.

According to the above results, the primitive effectiveness of both the phase indexer and correlation measure of the proposed method has been sufficiently checked.

3.2 Flight characteristics estimation

In order to evaluate the effectiveness of the proposed method, especially, the phase indexer, lift C_L and drag C_D coefficients of “Hisho” are estimated. The lift and drag coefficients are important aerodynamics parameters to determine aircraft performance, and their accurate estimation by using flight data is also required. Generally, to estimate these parameters, special flight tests in which disturbance represented by gust is reduced as much as possible are conducted. Thus, in order to test the capability of the method, the category B flight data, which does not suit for the use of the estimation directly, is selected as the source data for the estimation.

Figure 6 is the results estimated with parts of the category B flight data recognized as stable by the method. The results are indicated in the form of lift curve and drag polar, that is, the horizontal axes show the angle of attack α and drag coefficient C_D , respectively, while both the vertical axes illustrate the lift coefficient C_L . The estimation is performed sample by sample, and the results are also shown sample by sample as the

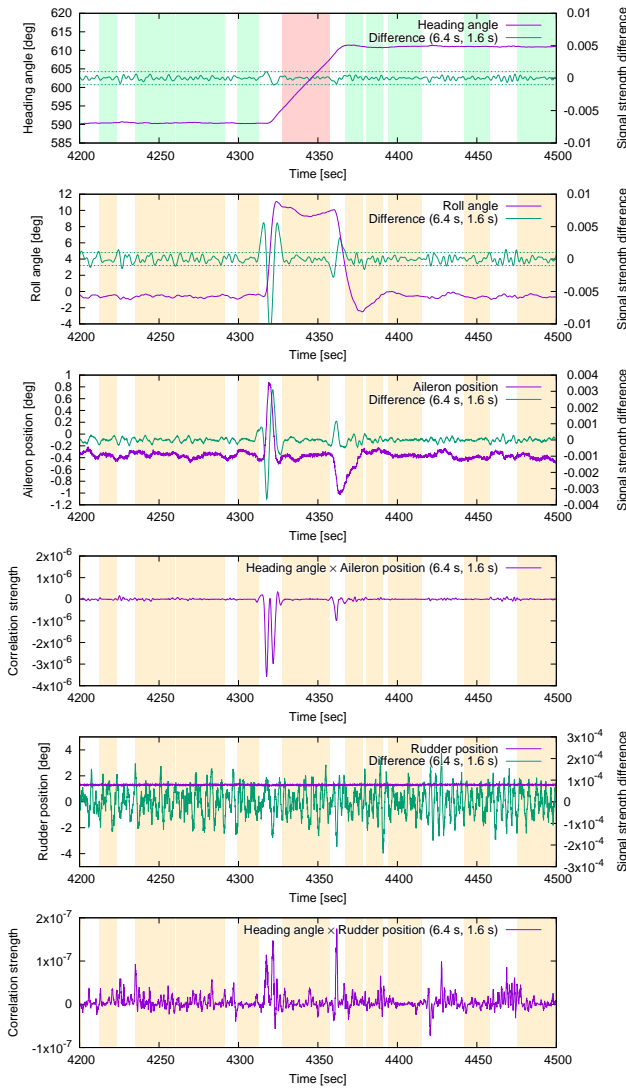


Fig. 5 Example correlation measurement of heading and aileron position

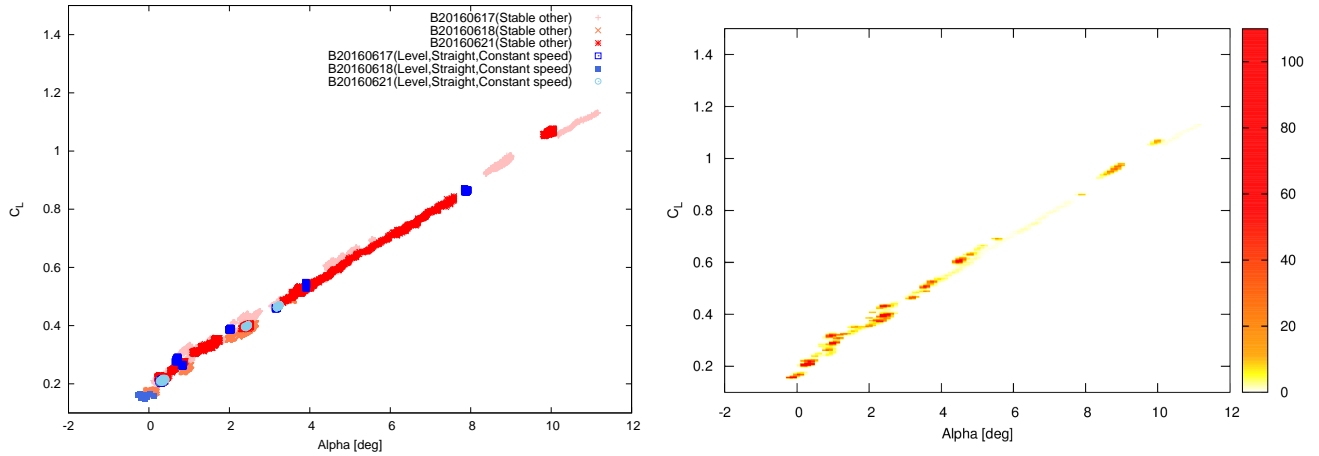
left graphs. In addition to these graphs, the right graphs are their histogram, which depict the density of the results.

Based on the information obtained with the phase indexer of the proposed method, the results are divided into two categories; the source data belongs to the level, straight, constant airspeed phase, or the other phases. According to Fig. 6, both the category results are reasonable, because the lift curve and drag polar represent linear and parabolic relations. However, there is difference; the results obtained with the level, straight and constant airspeed phase are concentrated on several points, while those of the other phases are spread. This fact supports the capability of the phase indexer. If a goal of the estimation requires statistical accuracy, for example, comparison of flight test results with other results of wind tunnel test results and computational fluid dynamics calculation at design validation stage, the level, straight, constant airspeed phase will be suitable to be selected. On the other hands, when there is another goal to obtain overall characteristics covering flight envelop thoroughly such as modeling for flight simulator, the other phase results will also be utilized. Therefore, it is concluded that the proposed method, especially, the phase indexer is effective for flight characteristics estimation.

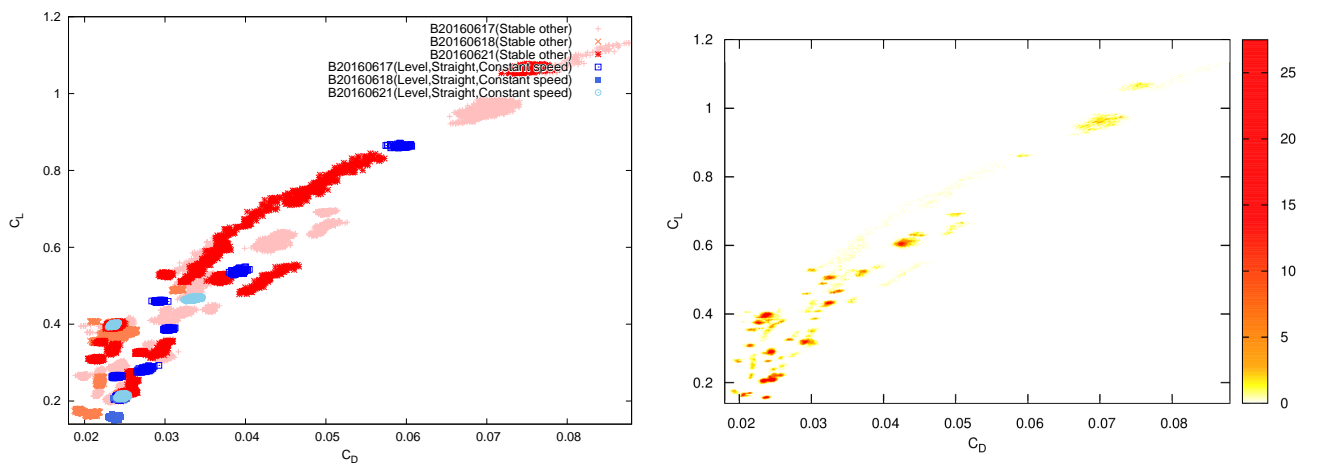
3.3 Abnormal detection

The second demonstration is abnormal detection. For the demonstration, the category B flights are focused again. In the category B flights, the dutchroll motion, which is abnormal in ordinary flight, is intentionally invoked many times for experimental purpose by applying doublet input to the rudder pedals. Figure 7 shows the time histories of heading, roll angle, rudder position with its correlation strength to heading. It corresponds to the red dashed box area of Fig. 4. Compared to the normal turn case shown in Fig. 5, the correlation strength between heading and rudder position takes far larger values.

By utilizing the correlation strength, dutchroll maneuvering in the category B flights is detected as a demonstrative fault detection



(a) Lift curve



(b) Drag polar

Fig. 6 Lift curve and drag polar estimated with the stable data extracted from the category B flights, left and right graphs are plotted sample by sample and in the form of data density, respectively.

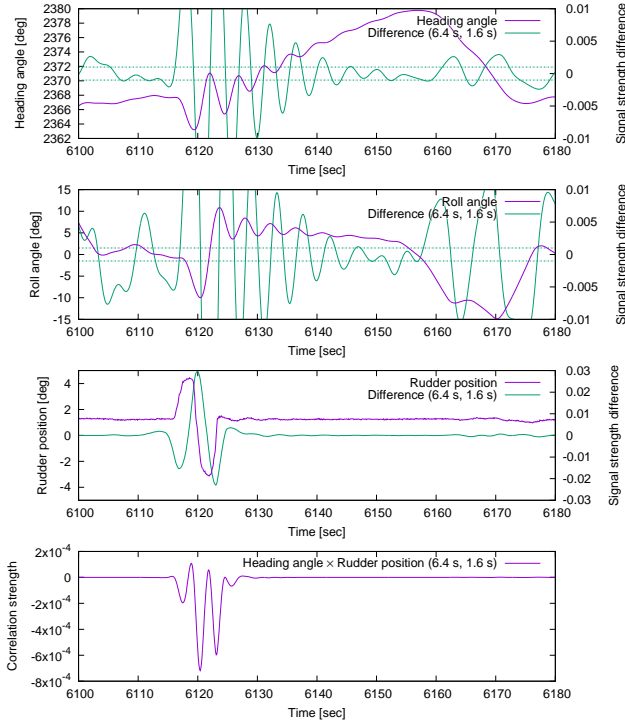


Fig. 7 Dutchroll in category B flight

application. Figure 8 indicates the time histories of the correlation strength in the all three category B flights. The numbers of occurrence of the comparative strong correlation in flight, which excludes the first and last cases recorded on ground, are 6, 8, and 7 for flight No. B160617, B160618, and B160621, respectively. These values are confirmed to be exactly identical to the numbers of trials. Therefore, it can be concluded that the proposed method will be useful for fault detection applications.

4 Conclusion

This paper describes the new flight data preprocessing method. The method add the flight data in the form of time series data to the indexes representing the flight phases. It also measures the correlation strength of the multiple kinds of the flight data.

The goal of the method is to provide useful information especially for the two application; flight characteristics estimation and fault detection. The capability of the proposed method has been demonstrated with the real flight data. Applying the method to the normal and experimen-

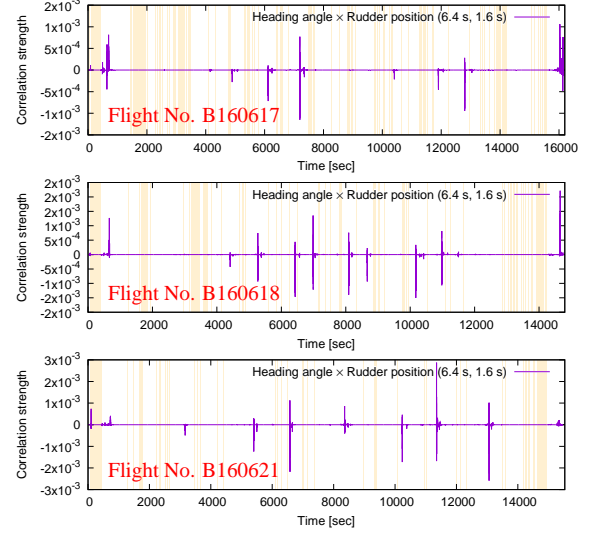


Fig. 8 Correlation strength between heading and rudder in category B flights

tal flights clearly characterizes the two category flights, which shows the primitive effectiveness of the method. For the demonstration of the flight characteristics estimation, the phase indexer capability has been shown based on the comparisons with the lift and drag coefficients estimated by using the level, straight, constant airspeed phase and other phase data. The dutchroll invoked intentionally as abnormal motion has been successfully detected with the correlation measure functionality of the proposed method.

According to the results, it can be concluded that the comprehensive effectiveness of the proposed method has been successfully checked. It is noted that this work was supported by JSPS KAKENHI Grant Number 15K06612.

References

- [1] M. Naruoka. Flight data classifier for effective aircraft performance analysis. In *ICAS2014, 29th International Congress of the Aeronautical Sciences, St.petersburg, Russia*, Sep 2014.
- [2] Stephane G. Mallat. A theory for multiresolution signal decomposition : the wavelet representation. *IEEE Transaction on Pattern Analysis and Machine Intelligence*, 1989.
- [3] Alfred Haar. Zur theorie der orthogonalen funktionensysteme. *Mathematische Annalen*, Vol. 69, No. 3, pp. 331–371, 1910.
- [4] H. Tomita, K. Masui, K. Hozumi, M. Naruoka,

A. Yokoyama, S. Sumii, S. Ito, T. Oshima, and N. Tanaka. A Network-Based Flight Data Acquisition System of the JAXA Flying Test Bed "Hisho". In *Proceedings of the 50th Aircraft Symposium*, pp. 2819–2827, Nov. 2012. 2B07 (in Japanese).

Contact Author Email Address

naruoka.masaru@jaxa.jp

Copyright Statement

The authors confirm that they, and/or their company or organization, hold copyright on all of the original material included in this paper. The authors also confirm that they have obtained permission, from the copyright holder of any third party material included in this paper, to publish it as part of their paper. The authors confirm that they give permission, or have obtained permission from the copyright holder of this paper, for the publication and distribution of this paper as part of the ICAS proceedings or as individual off-prints from the proceedings.